AN AMPLIFICATION FACTOR TO ENHANCE STABILITY FOR STRUCTURE-DEPENDENT INTEGRATION METHOD

S.-Y. Chang *

Department of Civil Engineering
National Taipei University of Technology
Taipei, Taiwan 10608, R.O.C.

ABSTRACT

Chang explicit method (2007) has been shown to be unconditionally stable for a linear elastic system and any instantaneous stiffness softening system while it is only conditionally stable for any instantaneous stiffness hardening system. Its coefficients of the difference equation for displacement increment are functions of initial tangent stiffness. Since Chang explicit method is unconditionally stable for a linear elastic system and any instantaneous stiffness softening system, its stability range can be enlarged if the initial tangent stiffness is enlarged by an amplification factor and then this amplified initial tangent stiffness is used to determine the coefficients. The detailed implementation of this scheme for Chang explicit method is presented and the feasibility of this scheme is verified.

Keywords: Dynamic analysis, Time integration, Stability, Accuracy, Structure-dependent method.

1. INTRODUCTION

The most important advantage of an explicit method (Newmark [1]; Shing and Mahin [2]; Chang [3,4]) is the explicitness of each time step while that for an implicit method (Houbolt [5]; Newmark [1]; Wilson *et al*. [6]; Park [7]; Hilber *et al*. [8]; Wood *et al*. [9]; Chung and Hulbert [10]; Chang [11]) is the possibility of unconditional stability. It has been shown that Chang explicit method (2002, 2007) is explicit and has unconditional stability for a linear elastic system and any instantaneous stiffness softening system. However, it can only possess conditional stability for an instantaneous stiffness hardening system. Apparently, a promising improvement for this integration method is to extend the unconditional stability to an instantaneous stiffness hardening system.

Chang explicit method (CEM) is promising in the step-by-step solution of a general structural dynamic problem, where the total response is dominated by the low frequency modes while the high frequency responses are of no interest. However, its practical applications might be inconvenient or limited due to the only conditional stability for an instantaneous stiffness hardening system. In order to improve its stability properties, an amplification factor is introduced to amplify the initial tangent stiffness and then the amplified initial tangent stiffness is used to replace the initial tangent stiffness to determine the coefficients of the difference equation for displacement increment. The detailed implementation of this scheme for CEM will be presented first and will lead to a new integration method. Apparently, this integration method is modified from Chang explicit method and thus will be referred as modified Chang explicit method (MCM) for brevity. Subsequently, the numerical properties of MCM in the step-by-step solution of a linear elastic system and a nonlinear system will be analytically explored. Finally, some numerical examples are applied to confirm the analytical results.

2. MODIFIED CHANG EXPLICIT METHOD

For CEM, the coefficients of the difference equation for displacement increment are generally determined from the mass, initial tangent stiffness and step size. Since the numerical properties of CEM are closely related to these coefficients, a slight modification of these coefficients might lead to improved stability properties. In order to conceptually illustrate the feasibility of the proposed scheme, the instantaneous degree of nonlinearity δ_{i+1} needs to be described first. This parameter is used to monitor the stiffness change and is defined as

$$\delta_{i+1} = \frac{k_{i+1}}{k_0} \tag{1}$$

where δ_{i+1} is the ratio of the instantaneous stiffness k_{i+1} at the end of the $(i+1)-th$ time step over the initial tangent stiffness k_0. It is implied by $\delta_{i+1} = 1$ that the instantaneous stiffness at the end of the $(i+1)-th$ time step is equal to the initial stiffness. Whereas, $\delta_{i+1} > 1$ denotes the case of stiffness hardening for the instanta-

* Corresponding author (changsy@ntut.edu.tw)

DOI : 10.1017/jmech.2012.103
Copyright © 2012 The Society of Theoretical and Applied Mechanics, R.O.C.
https://doi.org/10.1017/jmech.2012.103 Published online by Cambridge University Press

neous stiffness at the end of the $(i+1)-th$ time step when referring to the initial stiffness and the case of stiffness softening can be represented by $0 < \delta_{i+1} < 1$.

It has been shown by Chang [12] that CEM is unconditionally stable as $\delta_{i+1} = k_{i+1} / k_0 \le 1$. Hence, the value of δ_{i+1} will be decreased if the initial tangent stiffness k_0 is multiplied by an amplification factor σ. As a result, the instantaneous degree of nonlinearity will change from δ_{i+1} to δ_{i+1} / σ. This implies that unconditional stability can be achieved if $\delta_{i+1} / \sigma \le 1$ is met. Based on this scheme, the formulation of MCM for a single degree of freedom system can be expressed as

$$\begin{aligned} & m a_{i+1} + c v_{i+1} + k d_{i+1} = f_{i+1} \\ & d_{i+1} = d_i + \beta_1 (\Delta t)\, v_i + \beta_2 (\Delta t)^2 a_i \\ & v_{i+1} = v_i + \frac{1}{2}(\Delta t)(a_i + a_{i+1}) \end{aligned} \tag{2}$$

where m, c, k and f are the mass, viscous damping coefficient, stiffness and external force, respectively. After introducing the parameter σ into the coefficients β_1 and β_2, they are found to be

$$\beta_1 = \frac{1 + \xi\Omega_0}{1 + \xi\Omega_0 + \frac{1}{4}\sigma\Omega_0^2}, \quad \beta_2 = \frac{\frac{1}{2}}{1 + \xi\Omega_0 + \frac{1}{4}\sigma\,\Omega_0^2} \tag{3}$$

where ξ represents the viscous damping ratio and $\Omega_0 = \omega_0(\Delta t)$; and $\omega_0 = \sqrt{k_0 / m}$ is the natural frequency of the system determined from the initial stiffness k_0. It is apparent that MCM will reduce to CEM if $\sigma = 1$ is adopted. This implies that MCM with $\sigma = 1$ is CEM. As a summary, the major concept of this scheme is to visually increase the initial stiffness so that the instantaneous degree of nonlinearity is less than or equal to 1 since CEM is unconditionally stable for a linear elastic system and any instantaneous stiffness softening system.

It is important for computational efficiency to rewrite $\xi\Omega_0$ and Ω_0^2 in terms of the initial structural properties and the time step based on the fundamental theory of the structural dynamics. This is because that the expressions of $\xi\Omega_0$ and Ω_0^2 will involve solving an eigenvalue problem, which is time consuming for a multiple degree of freedom system with matrices of larger order. As a result, the coefficients β_1 and β_2 can be rewritten as

$$\begin{aligned} \beta_1 &= \frac{m + \frac{1}{2}(\Delta t)c}{m + \frac{1}{2}(\Delta t)\, c + \frac{1}{4}(\Delta t)^2 \sigma k_0}, \\ \beta_2 &= \frac{\frac{1}{2}m}{m + \frac{1}{2}(\Delta t)\, c + \frac{1}{4}(\Delta t)^2\, \sigma k_0} \end{aligned} \tag{4}$$

where $c = 2\xi\omega_0 m$, which is assumed that the viscous damping ratio is determined from the initial structural properties. Thus, the coefficients β_1 and β_2 are not constants but depend on the initial structural properties and the step size. These coefficients are proposed to be invariant in a complete step-by-step integration procedure in the original development of this integration method.

3. COMPUTING SEQUENCE IN SINGLE TIME STEP

In order to evaluate the numerical properties of MCM in the solution of linear elastic and nonlinear systems, its computing sequence for a single time step must be reflected in the analysis. The stiffness in the first line of Eq. (2) might vary not only from step to step but also within a time step for a nonlinear system. Hence, this characteristic must be considered in the basic analysis. For this purpose, r_i is used to represent the restoring force at the end of the $(i)-th$ time step and is expressed as, $r_i = k_i\, d_i$, where k_i is the stiffness at the end of the $(i)-th$ time step.

Because the acceleration, velocity and displacement at the $(i)-th$ time step are available at the start of the $(i+1)-th$ time step, the displacement d_{i+1} can be computed from the second line of Eq. (2). Subsequently, the restoring force r_{i+1} corresponding to the displacement d_{i+1} is determined from an assumed force-displacement relation and is expressed as $r_{i+1} = k_{i+1}\, d_{i+1}$. Next, after substituting the acceleration a_{i+1}, which is expressed as a function of v_{i+1} by using the third line of Eq. (1), into the first line of Eq. (1), the velocity v_{i+1} is found to be

$$v_{i+1} = \left[m + \frac{c(\Delta t)}{2} \right]^{-1} \left[m v_i + \frac{1}{2}(\Delta t)\, m a_i + \frac{1}{2}(\Delta t)(f_{i+1} - k_{i+1}\, d_{i+1}) \right] \tag{5}$$

Finally, the first line of Eq. (1) is employed to compute the acceleration a_{i+1}. This computing sequence for the $(i+1)-th$ time step can be rewritten in a recursive matrix form and is

$$\mathbf{X}_{i+1} = \mathbf{A}_{i+1}\, \mathbf{X}_i + \mathbf{L}_{i+1}\, f_{i+1} \tag{6}$$

where $\mathbf{X}_{i+1} = \left[d_{i+1},\ (\Delta t) v_{i+1},\ (\Delta t)^2 a_{i+1} \right]^{\mathrm{T}}$ is defined, and the symbols $\mathbf{A}_{i+1}$ and $\mathbf{L}_{i+1}$ represent the amplification matrix and the load factor for the $(i+1)-th$ time step, respectively.

4. BASIC ANALYSIS

In order to facilitate the basic analysis, it is needed to derive the explicit expression of the amplification matrix $\mathbf{A}_{i+1}$ for MCM. As a result, it is found to be

https://doi.org/10.1017/jmech.2012.103 Published online by Cambridge University Press

$$\mathbf{A}_{i+1}=\begin{bmatrix} 1 & \dfrac{1+\xi\Omega_0}{1+\xi\Omega_0+\dfrac{1}{4}\sigma\Omega_0^2} & \dfrac{\dfrac{1}{2}}{1+\xi\Omega_0+\dfrac{1}{4}\sigma\Omega_0^2} \\ \dfrac{-\dfrac{1}{2}\Omega_{i+1}^2}{1+\xi\Omega_0} & \dfrac{1}{1+\xi\Omega_0}-\dfrac{\dfrac{1}{2}\Omega_{i+1}^2}{1+\xi\Omega_0+\dfrac{1}{4}\sigma\Omega_0^2} & \dfrac{\dfrac{1}{2}}{1+\xi\Omega_0}-\dfrac{\dfrac{1}{4}\Omega_{i+1}^2}{(1+\xi\Omega_0)\left(1+\xi\Omega_0+\dfrac{1}{4}\sigma\Omega_0^2\right)} \\ \dfrac{-\Omega_{i+1}^2}{1+\xi\Omega_0} & \dfrac{-2\xi\Omega_0}{1+\xi\Omega_0}-\dfrac{\Omega_{i+1}^2}{1+\xi\Omega_0+\dfrac{1}{4}\sigma\Omega_0^2} & \dfrac{-\xi\Omega_0}{1+\xi\Omega_0}-\dfrac{\dfrac{1}{2}\Omega_{i+1}^2}{(1+\xi\Omega_0)\left(1+\xi\Omega_0+\dfrac{1}{4}\sigma\Omega_0^2\right)} \end{bmatrix}$$

$$\mathbf{L}_{i+1}=\left(\frac{1}{k_{i+1}}\right)\left(\frac{\Omega_{i+1}^2}{1+\xi\Omega_0}\right)\begin{bmatrix}0\\ \dfrac{1}{2}\\ 1\end{bmatrix} \tag{7}$$

The characteristic equation for the amplification matrix of $\mathbf{A}_{i+1}$ can be further derived from the equation of $|\,\mathbf{A}_{i+1}-\lambda\mathbf{I}\,|=0$, which gives

$$\lambda^3-A_1\lambda^2+A_2\lambda-A_3=0 \tag{8}$$

where λ represents an eigenvalue of the matrix $\mathbf{A}_{i+1}$; and the explicit expressions of A_1, A_2 and A_3 are found to be

$$\begin{aligned} A_1&=\frac{2}{1+\xi\Omega_0}-\frac{\left(1+\dfrac{1}{2}\xi\Omega_0\right)\Omega_{i+1}^2}{(1+\xi\Omega_0)\left(1+\xi\Omega_0+\dfrac{1}{4}\sigma\Omega_0^2\right)}\\ A_2&=\frac{1-\xi\Omega_0}{1+\xi\Omega_0}+\frac{\dfrac{1}{2}\xi\Omega_0\,\Omega_{i+1}^2}{(1+\xi\Omega_0)\left(1+\xi\Omega_0+\dfrac{1}{4}\sigma\Omega_0^2\right)}\\ A_3&=0 \end{aligned} \tag{9}$$

Using this characteristic equation, numerical properties of MCM can be evaluated and compared to those of CEM.

4.1 Stability

It is generally recognized that a stable computation, which leads to either an exponential decay or a bounded oscillatory response, requires the absolute eigenvalues of $\mathbf{A}_{i+1}$ smaller than or equal to 1 (Belytschko and Hughes [13], Hughes [14], Zienkicwicz [15]). This leads to

$$\begin{matrix}-1\le A_2\le 1\\ -(A_2+1)\le A_1\le(A_2+1)\end{matrix}\quad\text{or}\quad\begin{matrix}A_2=1\\ -2\le A_1\le 2\end{matrix} \tag{10}$$

After substituting the coefficients of A_1, A_2 and A_3, as shown in Eq. (9), into this equation, the stability conditions is found to be

$$\begin{aligned} &0<\Omega_0\le\infty && \text{if}\quad \delta_{i+1}\le\sigma\\ &0<\Omega_0\le\frac{2\xi+2\sqrt{\xi^2+(\delta_{i+1}-\sigma)}}{\delta_{i+1}-\sigma} && \text{if}\quad \delta_{i+1}>\sigma \end{aligned} \tag{11}$$

for MCM. This equation reveals that MCM has unconditional stability as $\delta_{i+1}\le\sigma$ while it is only conditionally stable as $\delta_{i+1}>\sigma$.

It is advisable to meet a slightly more stringent stability condition by restricting the eigenvalues of the amplification matrix to be complex conjugate in addition to the condition of $|\,\lambda_{1,2}\,|\le 1$. These will result in

$$(A_1)^2-4A_2\le 0\quad\text{and}\quad 0\le A_2\le 1 \tag{12}$$

As a result, the stability conditions for MCM are found to be

$$\begin{aligned} &0<\Omega_0\le\frac{2\sqrt{\delta_{i+1}-\xi^2}\left(\sqrt{\delta_{i+1}-\xi^2}+\sqrt{\sigma-\xi^2}\right)}{\xi(\sigma-\delta_{i+1})} && \text{if}\quad \delta_{i+1}<\sigma\\ &0<\Omega_0\le\infty && \text{if}\quad \delta_{i+1}=\sigma\\ &0<\Omega_0\le\frac{2\xi+2\sqrt{\xi^2+(\delta_{i+1}-\sigma)}}{\delta_{i+1}-\sigma} && \text{if}\quad \delta_{i+1}>\sigma \end{aligned} \tag{13}$$

where $0\le\xi\le\sqrt{\delta_{i+1}}$ is needed as $\delta_{i+1}<\sigma$. The satisfaction of this equation guarantees a bounded oscillatory response, which excludes the response in the form of exponential decay. For zero viscous damping, Eqs. (11) and (13) both reduce to

$$\begin{aligned} &0<\Omega_0\le\infty && \text{if}\quad \delta_{i+1}\le\sigma\\ &0<\Omega_0\le\frac{2}{\sqrt{\delta_{i+1}-\sigma}} && \text{if}\quad \delta_{i+1}>\sigma \end{aligned} \tag{14}$$

This equation reveals that MCM is unconditionally stable for $\delta_{i+1}\le\sigma$ while it is conditionally stable for $\delta_{i+1}>\sigma$. This implies that the stability properties are improved if $\sigma>1$ is chosen.

https://doi.org/10.1017/jmech.2012.103 Published online by Cambridge University Press

In order to gain an insight into the stability conditions of MCM, The variations of upper stability limits with δ_{i+1} for some selected σ and for some specified ξ are plotted in Fig. 1. In each plot of Fig. 1, it is found that there is no upper stability limit as $\delta_{i+1} \le \sigma$ for zero viscous damping while it decreases from infinity to zero as δ_{i+1} increases from σ to infinity. Meanwhile, the upper stability limit almost increases from zero to infinity as δ_{i+1} increases from ξ^2 to σ for nonzero viscous damping. Furthermore, the upper stability limit decreases with the increase of the viscous damping ratio for a given δ_{i+1} in the range of $\delta_{i+1} \le \sigma$. As $\delta_{i+1} > \sigma$, the curve for the variation of upper stability limit with δ_{i+1} for nonzero viscous damping is similar to that for zero viscous damping. The upper stability limit slightly increases with an increasing viscous damping ratio for a given δ_{i+1} in the range of $\delta_{i+1} > \sigma$ since the three curves are almost overlapped together for $\xi = 0$, 0.1 and 0.2. Equation (13) reveals that MCM has unconditional stability in the range of $\delta_{i+1} \le \sigma$ if $\xi = 0$ while it becomes conditional stability if $\xi \ne 0$.

It is found from the comparisons of the four plots of Fig. 1 that the unconditional stability range increases from 1 to 2.5 as the amplification factor σ is increased from 1 to 2.5. This reveals that the stability properties will be improved if σ is chosen to be greater than 1. In addition, the larger the value of σ, the larger the unconditional stability range for a zero viscous damping ratio. However, it is needed to consider the other numerical properties for choosing an appropriate value of σ if they are affected by the increasing value of σ. It is very important to conclude that the use of the amplification factor σ for MCM can simply shift the bifurcation upper stability range from 1 to a specified value of σ, where the bifurcation upper stability range implies that unconditional stability bifurcate into conditional stability.

4.2 Numerical Dissipation and Period Distortion

If there are two complex conjugate eigenvalues at the $(i + 1)$–*th* time step for MCM, they can be computed from Eq. (8) and are found to be

$$\lambda_{1,2} = \frac{1}{2}A_1 \pm j\sqrt{A_2 - \frac{1}{4}A_1^2} = e^{-\bar{\xi}\bar{\Omega}_{i+1} \pm j\bar{\Omega}_{i+1}^D} \tag{15}$$

where $j = \sqrt{-1}$, $\bar{\Omega}_{i+1} = \bar{\omega}_{i+1}(\Delta t)$ and $\bar{\Omega}_{i+1}^D = \bar{\Omega}_{i+1}\sqrt{1-\xi^2}$. In addition, the damped phase angle $\bar{\Omega}_{i+1}^D$ and the numerical damping ratio $\bar{\xi}_{i+1}$ can be further obtained from this equation and are found to be

$$\bar{\Omega}_{i+1}^D = \tan^{-1}\sqrt{\frac{4A_2}{A_1^2} - 1}, \quad \bar{\xi}_{i+1} = -\frac{\ln(A_2)}{2\bar{\Omega}_{i+1}} \tag{16}$$

where $\bar{\xi}_{i+1}$ is a measure of numerical dissipation. The relative period error is usually employed to measure period distortion for a step-by-step integration method and is defined as

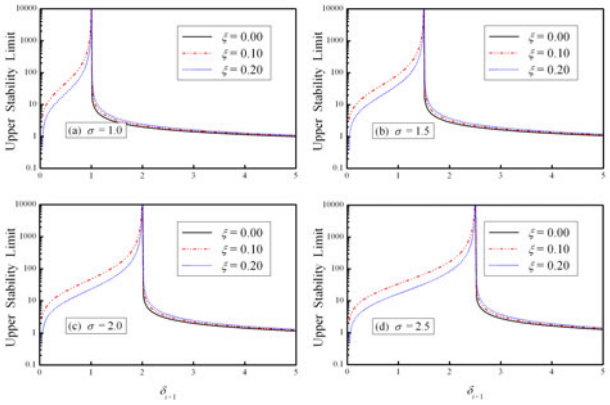


Fig. 1 Variation of upper stability limit with δ_{i+1}

$$P_{i+1} = \frac{\bar{T}_{i+1} - T_{i+1}}{T_{i+1}} = \frac{\omega_{i+1}}{\bar{\omega}_{i+1}} - 1 \tag{17}$$

where $\bar{T}_{i+1} = (2\pi)/\bar{\omega}_{i+1}$ and $T_{i+1} = (2\pi)/\omega_{i+1}$ represent the computed and true periods of the system, respectively. It is clear that $\bar{\xi}_{i+1}$ and $\bar{\omega}_{i+1}$ can be considered as the quantities corresponding to ξ_{i+1} and ω_{i+1} in a numerical solution.

The variations of the relative period errors with $\Delta t/T_0$, where $T_0 = 2\pi/\omega_0$, for MCM are shown in Fig. 2 for different instantaneous degree of nonlinearity δ_{i+1} and for σ = 1, 1.5, 2 and 2.5. In each curve of the four plots, the absolute relative period error increases with the increase of $\Delta t/T_0$ for a given δ_{i+1}. In Figs. 2(a) and 2(b), period is elongated for $\delta_{i+1} = 0.5$ and 1 for the four different σ values. However, period shrinkage is found for $\delta_{i+1} = 2$ and 3 as $\sigma = 2$, as shown in Figs. 2(c) and 2(d), although period elongation is also found in these two plots as σ = 1, 1.5 and 2. Period distortion seems relatively small as $\Delta t/T_0 \le 0.05$ in each curve of the four plots. This figure also reveals that period distortion increases with increasing σ for a given value of $\Delta t/T_0$ and the instantaneous degree of nonlinearity δ_{i+1} although this increase of σ value will improve the stability properties.

4.3 Spectral Radius

In general, the spectral radius of the amplification matrix of $\mathbf{A}_{i+1}$ is defined as the maximum absolute value of its eigenvalues and can be mathematically expressed as

$$\rho(\mathbf{A}_{i+1}) = \max|\lambda_k| \quad \text{for} \quad k = 1, 2, 3 \tag{18}$$

The closer $\rho(\mathbf{A}_{i+1})$ is to one the slower is the decay. Consequently, if it is desired that the high frequency responses be suppressed or even eliminated, $\rho(\mathbf{A}_{i+1})$ should be strictly less than one for these modes. Variations of spectral radii with $\Delta t/T_0$ for $\delta_{i+1} = 0.5$, 1, 2 and 3 for MCM are plotted in Fig. 3. In each plot of this figure, the spectral radius is always equal to 1 for MCM with $\sigma = 2$ and the constant average acceleration method (AAM) except that it will become very large

https://doi.org/10.1017/jmech.2012.103 Published online by Cambridge University Press

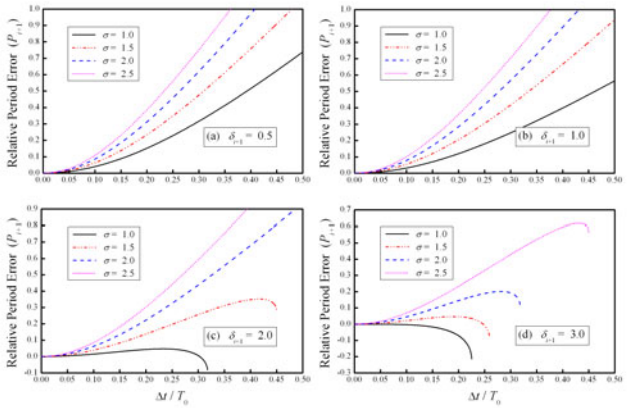


Fig. 2 Variation of relative period error with $\Delta t/T_0$ for zero viscous damping

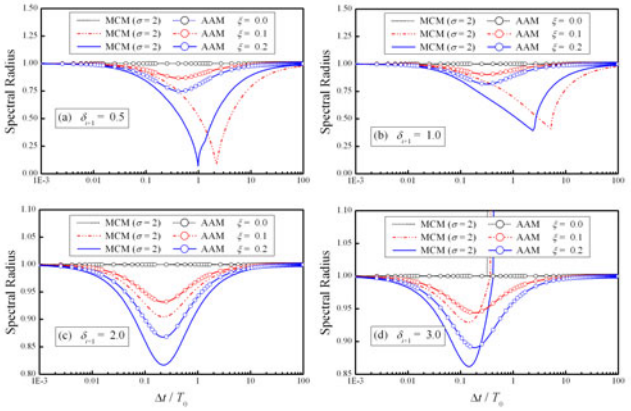


Fig. 3 Variation of spectral radius with $\Delta t/T_0$ for different viscous damping

after $\Delta t/T_0 > 1/\pi$ for the case of $\delta_{i+1} = 3$ in Fig. 3(d) for MCM with $\sigma = 2$. For the case of nonzero viscous damping, each curve starts from the spectral radius of 1, and then moves downward first and subsequently upward as the value of $\Delta t/T_0$ increases. Finally, the each curve converges to the spectral radius of 1 as $\Delta t/T_0$ is large enough. This indicates that the viscous damping is ineffective for suppressing or eliminating the high frequency modes.

4.4 Overshooting

To evaluate the tendency of an integration method to overshoot the exact solutions in the early response (Goudreau and Taylor [16]; Hilber and Hughes [17]) one can compute the free vibration response of a single degree of freedom system for the current time step based on the previous step data. Since only convergent methods are considered, there will be no overshoot as $\Omega_i \to 0$. The behavior as $\Omega_i \to \infty$ gives an indication of the behavior of the high frequency mode in a system where the values of $\Delta t/T_i$ are large for the high-frequency modes. The following equations are obtained from Eq. (6) for the limiting condition of $\Omega_i \to \infty$.

$$d_{i+1} \approx \left(1 - \frac{2\delta_i}{\sigma}\right) d_i$$
$$v_{i+1} \approx \left[-\frac{1}{2}(\delta_i + \delta_{i+1}) + \frac{\delta_i \delta_{i+1}}{\sigma}\right] \Omega_0^2 \left(\frac{d_i}{\Delta t}\right) + \left(1 - \frac{2\delta_{i+1}}{\sigma}\right) v_i \tag{19}$$

The first line of this equation reveals that MCM has no overshoot in displacement while it generally has a tendency to overshoot quadratically in Ω_i in velocity. For a linear elastic system, there is no overshoot in velocity for CEM since $v_{i+1} \approx (1 - 2/\sigma)v_i$ for $\delta_i = \delta_{i+1} = 1$, while overshooting is still found for MCM with $\sigma = 2$ since $v_{i+1} \approx -(\Omega_0^2/2)(d_i/\Delta t) + (1 - 2/\sigma)\, v_i$.

In order to numerically illustrate the overshooting characteristics of MCM, the free vibration response of a single degree of freedom system is computed by using MCM with $\sigma = 1$ and 2 with a relatively large time step, where MCM with $\sigma = 1$ also represents CEM. The stiffness is assumed to be in the following form so that a structural system with different stiffness properties can be simulated.

$$k = k_l(1 + \alpha u^2) \tag{20}$$

where u is the displacement degree of freedom and the stiffness consists of two parts. The linear part is represented by k_l while $\alpha u^2 k_l$ is the nonlinear part, which is displacement-dependent. The initial stiffness is found to be $k_0 = (1 + \alpha u_0^2)\, k_l$ based on the given initial conditions. The cases of $\alpha = -0.3$, 0 and 0.3 are used to simulate an instantaneous stiffness softening system, a linear elastic system and an instantaneous stiffness hardening system, respectively, in this numerical study. It is worth noting that the stiffness of $k = k_l(1 + \alpha u^2)$ must be always greater than 0 at any time instant for the single degree of freedom system.

An initial displacement of $d_0 = 1$ and a zero initial velocity of $v_0 = 0$ with $\Delta t/T_0 = 10$ are assumed for all the computations. The velocity term is normalized by the initial natural frequency of the system so that it can have the same unit as displacement. Numerical results obtained from MCM with $\sigma = 1$ and 2 are shown in Fig. 4. In addition, those obtained from AAM are also plotted in this figure for comparisons. There is no overshooting both in displacement and velocity for AAM for all the three different simulated systems. On the other hand, MCM with $\sigma = 1$ and 2 exhibits no overshooting in displacement for all the three different systems while an overshoot is generally found in velocity except for the case of the linear elastic system as shown in Fig. 4(e). It is worth noting that the results obtained from MCM with $\sigma = 1$ for the instantaneous stiffness hardening system blow up very early due to the violation of the upper stability limit. This is manifested from Figs. 4(c) and 4(f). It is manifested from Figs. 4(b) and 4(e) that the results obtained from the MCM with $\sigma = 1$ are exactly the same as those of AAM (Chang [12]). Thus, the phenomena of overshoot behaviors both in displacement and velocity for MCM are consistent with the analytical results shown in Eq. (19).

https://doi.org/10.1017/jmech.2012.103 Published online by Cambridge University Press

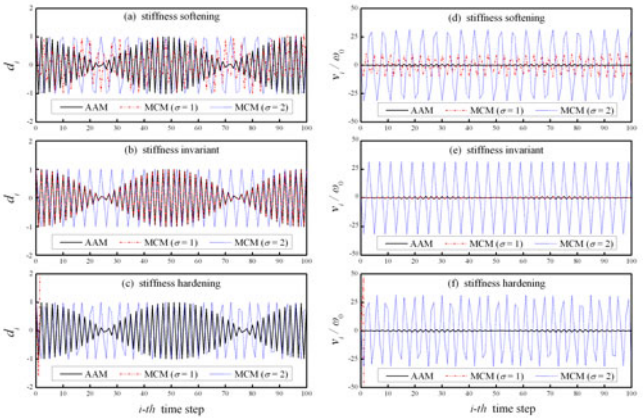


Fig. 4 Comparisons of overshoot responses

5. CHOICE OF APPROPRIATE AMPLIFICATION FACTOR

After investigating the numerical properties of MCM in the solution of linear elastic and nonlinear systems, it is found that for MCM with $\sigma > 1$, the larger the σ value, the larger the range to have unconditional stability. On the other hand, period distortion will increase with the increase of σ value for a given value of $\Delta t/T_0$ and a given instantaneous degree of nonlinearity. Hence, although a large value of σ ($\sigma > 1$) leads to better stability properties, it will sacrifice numerical accuracy. As a result, the guideline to select an appropriate amplification factor of σ for practical application is to consider an adequate unconditional stability range with an acceptable numerical accuracy.

Based on stability consideration, it seems appropriate to choose $\sigma = 2$ to have an adequate unconditional stability range for MCM since it has unconditional stability as $\delta_{i+1} \le 2$. Apparently, this stability range might be large enough for practical applications since it is very rare to see a structural system whose instantaneous stiffness can be as large as or greater than twice of the initial stiffness. On the other hand, in order to select an appropriate σ value for MCM based on accuracy consideration, the detailed values of the relative period errors as $\Delta t/T_0 = 0.05$ and 0.1 are listed in Table 1 for the σ values of 1, 1.5, 2 and 2.5. All these data are abridged from Fig. 2. It should be mentioned that the choice of $\Delta t/T \le 0.1$ (Clough and Penzien [18]) or 0.05 (Bathe [19]) has been suggested as a good rule of thumb for obtaining reliable results for linear elastic systems. It turns out this criterion will result in negligible amplitude growth or decay as well. Table 1 reveals that $\Delta t/T_0 = 0.1$ will result in too much period distortion for all the four σ values. Hence, it seems appropriate to choose a time step to meet $\Delta t/T_0 \le 0.05$ so that an acceptable numerical accuracy can be achieved. Among the four σ values in Table 1, it is found that MCM with $\sigma = 2$ will lead to the relative period errors of 2.26%, 2.06%, 1.64% and 1.21% in correspondence to $\delta_{i+1} = 0.5$, 1, 2 and 3 as $\Delta t/T_0 = 0.05$ is applied. This indicates that MCM can have an acceptable numerical accuracy if the value of $\sigma = 2$ is used.

Table 1 List of relative period error

	$\sigma = 1.0$		$\sigma = 1.5$		$\sigma = 2.0$		$\sigma = 2.5$	
	$\Delta t/T_0 = 0.05$	$\Delta t/T_0 = 0.1$	$\Delta t/T_0 = 0.05$	$\Delta t/T_0 = 0.1$	$\Delta t/T_0 = 0.05$	$\Delta t/T_0 = 0.1$	$\Delta t/T_0 = 0.05$	$\Delta t/T_0 = 0.1$
$\delta_{i+1} \le 0.5$	1.03%	4.02%	1.65%	6.36%	2.26%	8.66%	2.87%	10.90%
$\delta_{i+1} \le 1.0$	0.83%	3.20%	1.44%	5.57%	2.06%	7.88%	2.67%	10.14%
$\delta_{i+1} \le 2.0$	0.41%	1.50%	1.03%	3.91%	1.64%	6.26%	2.26%	8.56%
$\delta_{i+1} \le 3.0$	–0.02%	–0.31%	0.60%	2.15%	1.21%	4.55%	1.84%	6.89%

As a summary, the choice of $\sigma = 2$ for MCM seems to have an adequate unconditional stability range with an acceptable numerical accuracy for practical applications. MCM with $\sigma = 2$ can have the unconditional stability range of $\delta_{i+1} \le 2$ and it may cause a relative period error about 2% for a general structural system. It should be mentioned that to extend the unconditional stability range of $\delta_{i+1} \le 1$ for CEM to the range of $\delta_{i+1} \le 2$ for MCM with $\sigma = 2$ is important in practical applications. This is because that instability may occur for instantaneous stiffness hardening if using CEM since it only has conditional stability for an instantaneous stiffness hardening system. Hence, it might be needed to evaluate the system analyzed whether it experiences the case of instantaneous stiffness hardening. Consequently, the choice of a time step should meet the upper stability limit for an instantaneous stiffness hardening system. On the other hand, for MCM with $\sigma = 2$, the accuracy is the only consideration to have a reliable numerical solution since its unconditional stability range is as large as $\delta_{i+1} \le 2$, which is large enough for a general structural dynamic problem. In general, a very reliable solution can be obtained from MCM with $\sigma = 2$ if a time step is chosen to satisfy $\Delta t/T_0 \le 0.05$ for the modes of interest, which is manifested from Fig. 2. It should be mentioned that the capability to accurately capture dynamic loading is another consideration for obtaining an accurate solution and can be found in the references (Chang [20,21]; Chang *et al*. [22]).

6. MDOF IMPLEMENTATION

It is found from the analytical studies that the stability properties of MCM can be drastically improved. Therefore, it is very important to further examine its actual performance in the solution of an actual structural system. For this purpose, MCM is implemented for a multiple degree of freedom system, and it can be explicitly expressed as

$$\begin{aligned} &\mathbf{M}\mathbf{a}_{i+1} + \mathbf{C}\mathbf{v}_{i+1} + \mathbf{K}\mathbf{d}_{i+1} = \mathbf{f}_{i+1} \\ &\mathbf{d}_{i+1} = \mathbf{d}_i + \mathbf{B}_1(\Delta t)\mathbf{v}_i + \mathbf{B}_2(\Delta t)^2\mathbf{a}_i \\ &\mathbf{v}_{i+1} = \mathbf{v}_i + \frac{1}{2}(\Delta t)(\mathbf{a}_i + \mathbf{a}_{i+1}) \end{aligned} \tag{21}$$

https://doi.org/10.1017/jmech.2012.103 Published online by Cambridge University Press

where **K** is the stiffness matrix, **C** is the damping matrix and the coefficient matrices are

$$\mathbf{B}_1 = \left[\mathbf{M} + \frac{1}{2}(\Delta t)\,\mathbf{C}_0 + \frac{1}{4}(\Delta t)^2\sigma\mathbf{K}_0\right]^{-1}\left[\mathbf{M} + \frac{1}{2}(\Delta t)\,\mathbf{C}_0\right]$$
$$\mathbf{B}_2 = \left(\frac{1}{2}\right)\left[\mathbf{M} + \frac{1}{2}(\Delta t)\,\mathbf{C}_0 + \frac{1}{4}(\Delta t)^2\sigma\mathbf{K}_0\right]^{-1}\mathbf{M} \tag{22}$$

where $\mathbf{C}_0$ is the damping matrix, generally determined from the initial structural properties, and $\mathbf{K}_0$ is the initial stiffness matrix. In the first line of equation (21), a constant damping matrix is often assumed, *i.e.*, $\mathbf{C} = \mathbf{C}_0$., while the stiffness matrix **K** is generally different from the initial stiffness $\mathbf{K}_0$ for a nonlinear system.

In performing the step-by-step integration of the $(i + 1)$–*th* time step, the displacement vector $\mathbf{d}_{i+1}$ can be computed by the second line of Eq. (21). Next, the velocity vector is obtained from substituting the first line into the third line of Eq. (21) and is

$$\mathbf{v}_{i+1} = \left[\mathbf{M} + \frac{1}{2}(\Delta t)\,\mathbf{C}\right]^{-1}\left\{\mathbf{M}\left[\mathbf{v}_i + \frac{1}{2}(\Delta t)\,\mathbf{a}_i\right] + \frac{1}{2}(\Delta t)(\mathbf{f}_{i+1} - \mathbf{K}\mathbf{d}_{i+1})\right\} \tag{23}$$

Finally, the acceleration vector can be calculated by using the equation of motion as shown in the first line of Eq. (21).

The application of the second line of Eq. (21) to yield the displacement vector $\mathbf{d}_{i+1}$ can be alternatively implemented for brevity and it is numerically equivalent to solve the equation of

$$\left[\mathbf{M} + \frac{1}{2}(\Delta t)\,\mathbf{C}_0 + \frac{1}{4}(\Delta t)^2\sigma\mathbf{K}_0\right](\mathbf{d}_{i+1} - \mathbf{d}_i) = \left[\mathbf{M} + \frac{1}{2}(\Delta t)\,\mathbf{C}\right](\Delta t)\,\mathbf{v}_i + \frac{1}{2}\mathbf{M}(\Delta t)^2\mathbf{a}_i \tag{24}$$

Although MCM has an explicit implementation it requires solving this equation to yield the next step displacement vector. At first glance, it consumes more computational effort when compared to explicit methods since a triangulation and a substitution are needed if a direct elimination method is employed. However, the triangulation of the matrix of $[\mathbf{M} + 1/2(\Delta t)\mathbf{C}_0 + 1/4(\Delta t)^2\sigma\mathbf{K}_0]$ is needed to be conducted only once since it remains invariant for a whole step-by-step integration procedure. Similarly, $[\mathbf{M} + 1/2(\Delta t)\mathbf{C}_0]$ also needs to be triangulated once to determine the next step velocity vector if the viscous damping matrix is determined from the initial structural properties. Apparently, it involves no triangulation in determining the next step velocity vector if zero viscous damping is assumed and a lumped mass matrix is adopted. Hence, the computational efficiency is significantly improved since this triangulation consumes the most computational efforts per time step. In fact, MCM will involve commensurate computational efforts when compared to an explicit method.

7. NUMERICAL EXAMPLES

In order to confirm the numerical properties, such as stability and accuracy, of MCM for both linear elastic and nonlinear systems some numerical examples are considered next. In addition, the computational efficiency of this method is also studied in contrast to the Newmark explicit method (NEM) and AAM.

Example 1 --- Instantaneous Stiffness Invariant

A two-story shear-beam type structure is studied. The floor beams and slabs of the structure are assumed to be flexurally rigid. The lumped masses for the bottom and top floors are taken to be $m_b = 10^3$kg and $m_t = 10^4$kg, respectively. On the other hand, the stiffness of each story is taken to be in the form of

$$k = k_0\left[1 + \alpha\sqrt{|\Delta u|}\right] \tag{25}$$

where k_0 is the initial stiffness and Δu is a story drift. The nonlinearity arises from the story drift by choosing $\alpha \neq 0$. The initial stiffness is taken as $k_0 = 10^7$N/m for the bottom story while for the top story it is taken to be $k_0 = 10^5$N/m. The natural frequencies of the structure are 3.15 and 100.50rad/sec based on the initial stiffness matrix. This structure is subjected to an acceleration of $3\sin(2t)$ at the base. The displacement response obtained from NEM with $\Delta t = 0.001$sec is considered as an "**exact**" solution for comparison. Meanwhile, numerical results are also obtained from MCM with $\sigma = 1$ and 2 for using $\Delta t = 0.05$sec.

The case of $\alpha = 0$ is taken in this example so that a linear elastic system can be simulated. Numerical results are shown in Fig. 5. The solutions obtained from MCM $\sigma = 1$ and 2 for using $\Delta t = 0.05$sec are reliable. This can be explained by Table 2, where the relative period error and the product of the natural frequency and time step for both modes are listed. The superscripts of (1) and (2) for P_i and Ω_0 represent the first and second modes, respectively. An unconditional stability is indicated by the numerical solutions obtained from MCM with $\sigma = 1$ and 2 with $\Delta t = 0.05$sec since it remains stable for the value of $\Omega_0^{(2)}$ as large as 5.03 for the second mode. The response contribution from the second mode to the total response is insignificant since reliable solutions are achieved for MCM with $\sigma = 1$ and 2 if using $\Delta t = 0.05$sec, where the first mode is reliably integrated while a very significant period distortion is found in the second mode. In fact, the relative period errors for the first mode are only 0.0021 and 0.0051 for MCM with $\sigma = 1$ and 2, respectively, while those for the second mode are 1.108 and 2.356, respectively.

Example 2 --- Instantaneous Stiffness Softening

To examine the performance of MCM in the solution of an instantaneous stiffness softening system, equation (25) is reconsidered for the same building by taking

https://doi.org/10.1017/jmech.2012.103 Published online by Cambridge University Press

Table 2 Some critical data for stability and accuracy

Method (step size)	$P_i^{(1)}$	$P_i^{(2)}$	$\Omega_0^{(1)}$	$\Omega_0^{(2)}$	$\Omega_0^{(u)}$
MCM with $\sigma = 1$ ($\Delta t = 0.05$)	0.0021	1.108	0.158	5.03	∞
MCM with $\sigma = 2$ ($\Delta t = 0.05$)	0.0051	2.356	0.158	5.03	∞

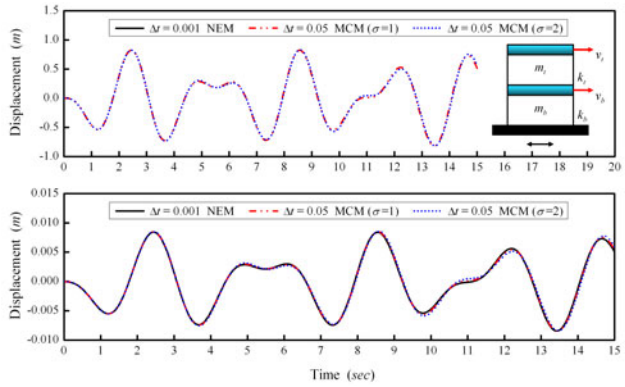


Fig. 5 Displacement responses for two-story shear-beam type structure (linear elastic)

$\alpha = -0.1$ and -0.2 for the bottom and top stories, respectively. Figure 6 shows the displacement responses. In addition, the response time histories of the relative period error, instantaneous degree of nonlinearity and upper stability limit are plotted in Fig. 7. Again, reliable solutions are still obtained from MCM with $\sigma = 1$ and 2 for using $\Delta t = 0.05$sec since the relative period error is small for the first mode, as shown in Fig. 7(a), although the second mode shows significant period distortion, as indicated in Fig. 7(b). Figures 7(c) and 7(d) reveal that the instantaneous degree of nonlinearity of both modes are always less than or equal to 1. Hence, a stable computation can be achieved for MCM with $\sigma = 1$ and 2 for using $\Delta t = 0.05$sec since they have unconditional stability for instantaneous stiffness softening systems. It is worth noting that no curves for MCM with $\sigma = 1$ and 2 for using $\Delta t = 0.05$sec in Figs. 7(e) and 7(f) are because that their upper stability limits are infinite.

Example 3 --- Instantaneous Stiffness Hardening System

Analytical results indicate that CEM will become conditionally stable as $\delta_{i+1} > 1$ while MCM with $\sigma = 2$ is unconditionally stable as $\delta_{i+1} \le 2$. Thus, this case is further confirmed next. For this purpose, Eq. (25) is also reused by choosing $\alpha = 10$ and 1 for the bottom and top stories, respectively. The displacement responses are shown in Fig. 8. In addition, the corresponding response time histories of relative period error, instantaneous degree of nonlinearity and upper stability limit are plotted in Fig. 9. It seems that only MCM with $\sigma = 2$ can give acceptable results. This is because that the relative period error is small for the dominant first mode, as shown in Fig. 9(a), although a very large

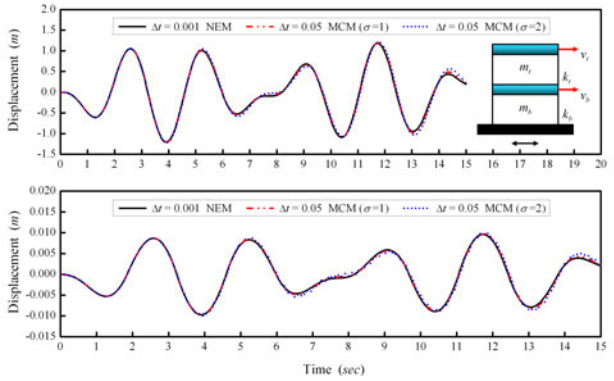


Fig. 6 Displacement responses for two-story shear-beam type structure (stiffness softening)

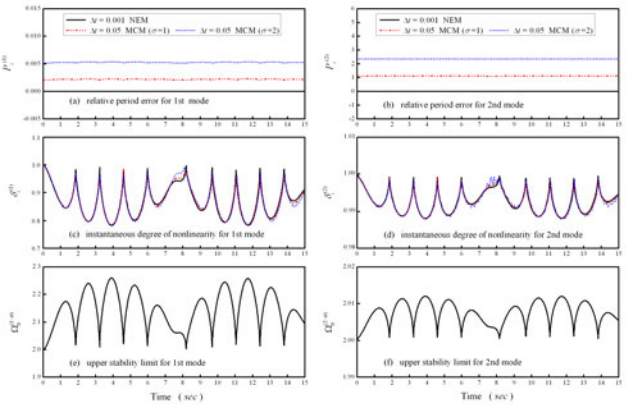


Fig. 7 Response time histories for two-story shear-beam type structure (stiffness softening)

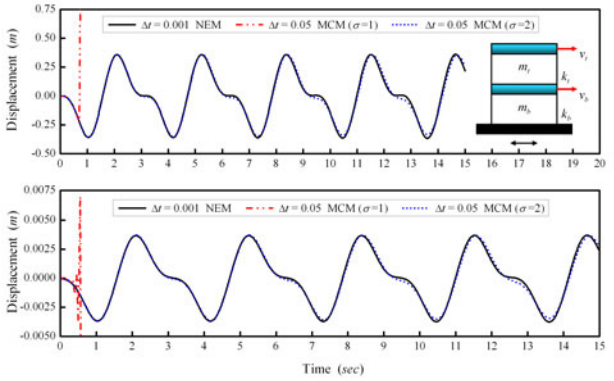


Fig. 8 Displacement responses for two-story shear-beam type structure (stiffness hardening)

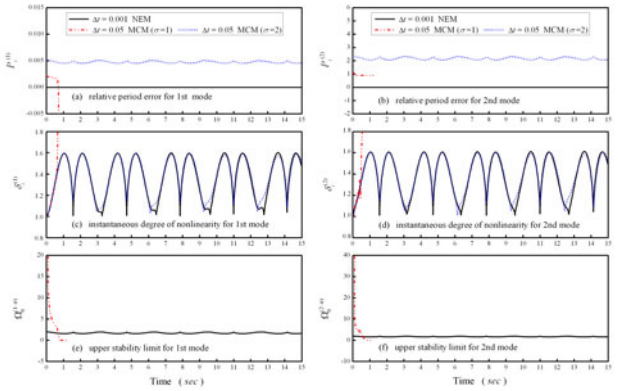


Fig. 9 Response time histories for two-story shear-beam type structure (stiffness hardening)

https://doi.org/10.1017/jmech.2012.103 Published online by Cambridge University Press

relative period error is found in the second mode, as shown in Fig. 9(b). However, the most important aspect is that MCM with $\sigma = 2$ is unconditionally stable as $\delta_{i+1} \le 2$ and both Figs. 9(c) and 9(d) show that $\delta_i^{(1)}$ and $\delta_i^{(2)}$ are less than about 2. Since both $\delta_i^{(1)}$ and $\delta_i^{(2)}$ are less than 2 there is no upper stability limit for MCM with $\sigma = 2$ as shown in Figs. 9(e) and 9(f). MCM with $\sigma = 1$ leading to instability is due to the violation of the upper stability limit as shown in Figs. 9(e) and 9(f) since it only has conditional stability as $\delta_{i+1} > 1$ and the instantaneous degree of nonlinearity is greater than 1 for each mode as shown in Figs. 9(c) and 9(d). This example reveals the superiority of MCM with $\sigma = 2$ over MCM with $\sigma = 1$ since it can have unconditional stability for an instantaneous stiffness hardening system.

Example 4 --- Fixed-Fixed Beam

In order to illustrate the most important improvement of MCM with $\sigma = 2$ in stability when compared to MCM with $\sigma = 1$, a fixed-fixed beam subject to a sine load at the center of the beam is considered. The dimension and structural properties of the steel beam are the sectional area of $6.0 \times 10^2 \text{mm}^2$, sectional modulus of $7.2 \times 10^3 \text{mm}^4$, length of $4.5 \times 10^3 \text{mm}$, Young's modulus of $2.0 \times 10^8 \text{N/mm}^2$ and density of $7.8 \times 10^{-6} \text{kg/mm}^3$. The steel beam was discretized with 10 beam elements and each node has the vertical and rotational degrees of freedom, resulting in a total of 18 degrees of freedom. A consistent mass matrix is used in the analysis and the material is assumed to be linearly elastic. Both the linear elastic stiffness matrix and the geometric stiffness matrix due to axial force are used to form the total stiffness matrix. Thus, the natural frequencies of this beam will vary with the change of the nonlinear stiffness matrix.

Using the initial stiffness matrix, the natural frequencies of the first three modes are found to be 19.38, 53.44 and 104.83rad/sec, and that for the last mode is 4180rad/sec. MCM with $\sigma = 1$ and 2 are used to solve the nonlinear problem. The response time histories at the center of the beam subject to the external force of $2.0 \times 10^5 \sin(\pi t)$N are plotted in Figs. 10 and 11. Fig. 10(a) exhibits the displacement response at the center of the fixed-fixed beam while the time histories of natural frequencies for the four modes are plotted in Fig. 11(b). In addition, the time histories of the upper stability limits are plotted in Fig. 11(c) for the four modes. On the other hand, the time histories of the relative period error, and instantaneous degree of nonlinearity for the first three modes and last mode are shown in Figs. 11(a), 11(b) and 11(c), respectively.

In Fig. 10(a), numerical results obtained from AAM with $\Delta t = 0.001$sec are considered as "**exact**" solutions for comparison. Accurate solutions are obtained from MCM with $\sigma = 2$ if a time step of $\Delta t = 0.005$sec is used while instability occurs for using MCM with $\sigma = 1$. To interpret these results it is of need to scrutiny the variations of structural properties with time. It is

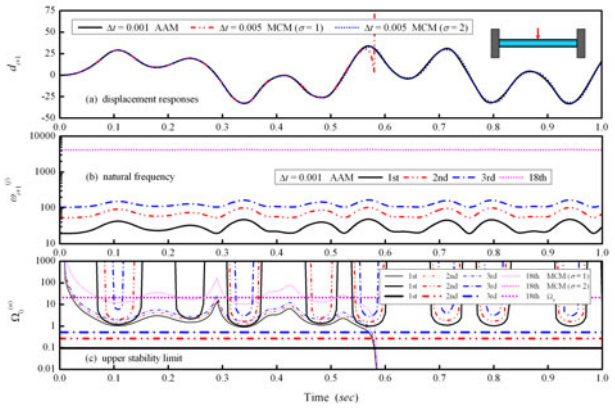


Fig. 10 Nonlinear response time histories at center of fixed-fixed beam for d_{i+1}, $\omega_{i+1}^{(f)}$ and $\Omega_0^{(u)}$

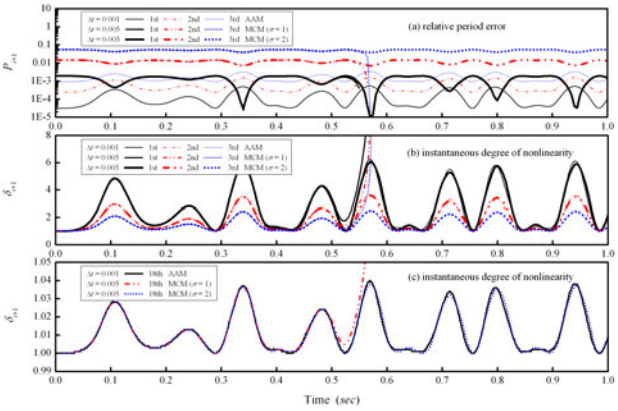


Fig. 11 Nonlinear response time histories at center of fixed-fixed beam for P_{i+1}, and δ_{i+1}

manifested from Fig. 10(b) that the natural frequencies of the first three modes vary with time significantly while they vary insignificantly for the last mode. This is consistent with Figs. 11(b) and 11(c). Figure 11(b) shows that δ_{i+1} roughly varies from 1 to 6, 1 to 3 and 1 to 2 for the first three modes, respectively, while it varies from 1 to 1.05 for the last mode as shown in Fig. 11(c). Thus, the first three modes experience significant instantaneous stiffness hardening while it is insignificant for the last mode. This might explain why MCM with $\sigma = 2$ can have reliable solutions and MCM with $\sigma = 1$ leads to instability. In Fig. 10(c), the upper stability limits for the four modes are plotted for MCM with $\sigma = 1$ and 2. In addition, the values of Ω_0 for the four modes are also plotted in this plot as straight lines to show if the upper stability limit is violated for each mode. It is clear that MCM with $\sigma = 1$ only has conditional stability for the four modes of this instantaneous stiffness hardening system since their upper stability limits are finite and tend to zero as instability occurs. It is found that the values of Ω_0 for the last mode may be greater than $\Omega_0^{(u)}$ for MCM with $\sigma = 1$ although those for the first three modes are less than $\Omega_0^{(u)}$. Thus, instability occurs. Whereas, MCM with $\sigma = 2$ is unconditionally stable for the last mode since its upper

https://doi.org/10.1017/jmech.2012.103 Published online by Cambridge University Press

stability limit is infinite and do not appear in this plot; and it remains stable for the first three modes since their values of Ω_0 are always less than $\Omega_0^{(u)}$.

Figure 11(a) reveals that the displacement response obtained from AAM for using a time step of Δt = 0.001sec is very accurate since the relative period errors for the first three modes are very small. For the solution obtained from MCM with σ = 2 for using Δt = 0.005sec, the average relative period errors for the first three modes are about 0.13%, 1.23% and 5.02%. Thus, the first mode is integrated very accurately and the second mode is integrated reliably while a considerable period distortion is found for the third mode. As a result, the solution seems accurate. This result indicates that a reliable solution can be achieved if the responses of the first and second modes are reliably integrated. Hence, the general concept to accurate integration of a linear elastic system, which requires that dominant modes be reliably integrated, may also be applied to a nonlinear system.

Example 5 --- Computational Efficiency

A n-degree-of-freedom spring-mass system is used to investigate the computational efficiency of MCM with σ = 2. This implies that a lumped mass matrix is adopted. Meanwhile, zero viscous damping is assumed for simplicity in the formulation of the equations of motion. As a result, only one triangulation is needed to determine the coefficient matrices in the step-by-step solution procedure. This example is intended to confirm that it involves much less computational efforts in obtaining a comparable solution when compared to AAM and NEM.

The structural properties of the spring-mass system are selected to be $m_i = 10^2$kg and $k_i = 10^8[1-(u_i - u_{i-1})^2]$N/m for $i = 1,\cdots, n$. The spring- mass system is excited by a harmonic load of sin(t). Three different systems are simulated by taking n = 500, 1000 and 2000. The lowest natural frequency is found to be 3.14rad/sec for the 500-DOF system before the system deforms. Similarly, it is found to be 1.57 and 0.785rad/sec for the 1000-DOF and 2000-DOF systems, respectively. Meanwhile, the highest natural frequency is found to be 2000.00rad/sec for the three systems. NEM, AAM and MCM with σ = 2 are applied to obtain the displacement responses. Since the highest natural frequency is as large as 2000.00rad/sec the time step of Δt = 0.001sec is chosen for the step-by-step integration based on stability consideration if using NEM. The numerical solution obtained from this time step is considered as an "**exact**" solution since the time step is much smaller than that required by accuracy consideration.

The displacement responses of the largest degree of freedom for the 500-DOF, 1000-DOF and 2000-DOF systems are shown in Fig. 12. MCM with σ = 2 and AAM give accurate solutions for the 500-DOF system if using Δt = 0.05sec. Meanwhile, both integration methods also lead to reliable results for the 1000-DOF system if using Δt = 0.10sec and for the 2000-DOF system if using Δt = 0.15sec. MCM with σ = 2 can have unconditional stability for instantaneous stiffness softening systems is strongly indicated by this example

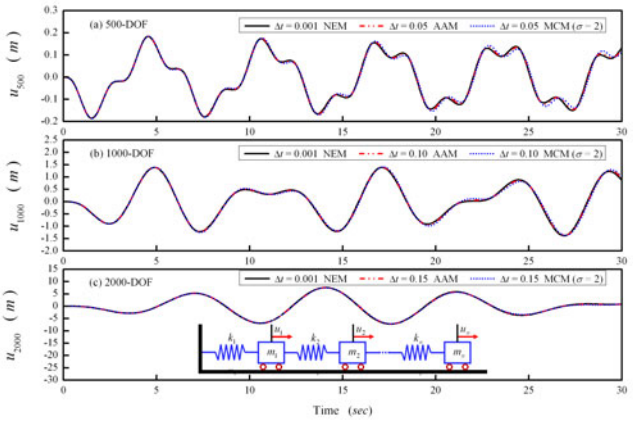


Fig. 12 Displacement responses for n-degree-of-freedom spring-mass system

since the product of the time step and the highest natural frequency is as large as 100 for the 500-DOF system, 200 for the 1000-DOF and 300 for the 2000-DOF system. It is inappropriate to use a conditionally stable, explicit method to solve a problem where high frequency responses contribute insignificantly to the total responses. However, it is illustrative to solve this problem by using NEM to emphasize the importance of the possibility of unconditional stability for MCM with σ = 2.

To compare the computational efficiency between NEM, AAM and MCM with σ = 2, the CPU time involved for each step-by-step analysis is recorded and summarized in Table 3. The CPU time consumed by NEM with Δt = 0.001sec is denoted by $\text{CPU}^{(\text{NEM})}$. Meanwhile, the symbols of $\text{CPU}^{(\text{AAM})}$ and $\text{CPU}^{(\text{MA})}$ are introduced to represent the CPU time consumed for using AAM and MCM with σ = 2. It is worth noting that the time step of 0.05sec is the largest allowable time step to yield reliable solutions for the 500-DOF system while those of 0.10sec and 0.15sec are for the 1000-DOf system and 2000-DOF system, respectively. The 4th column of Table 3 reveals that the modified algorithm with σ = 2 consumes the least CPU time for each system among the three integration methods, while both NEM and AAM involve much more computational efforts as shown in the 2nd and 3rd columns. It is generally recognized that NEM is computationally inefficient to solve this type of problems since it can only have conditional stability and thus the upper stability limit is a very stringent limitation in selecting an appropriate time step for the presence of the very high frequency of 2000rad/sec. In fact, a time step of Δt = 0.001sec is needed to meet the upper stability limit for the three different systems if using NEM. Meanwhile, although AAM can have unconditional stability and thus a large time step can be chosen based on accuracy consideration it still consumes many computational efforts. This is because that an iteration procedure is generally needed in each time step for an implicit method and it is very time consuming for a matrix of large order. Two attributes are responsible for the

https://doi.org/10.1017/jmech.2012.103 Published online by Cambridge University Press

Table 3 Comparison of CPU time

N-DOF	$CPU^{(NEM)}$	$CPU^{(AAM)}$	$CPU^{(MCM)}$	$CPU^{(MCM)}/CPU^{(NEM)}$	$CPU^{(MCM)}/CPU^{(AAM)}$
500	351.16	274.75	8.55	0.024	0.031
1000	1761.02	1684.77	22.83	0.013	0.014
2000	7191.33	11559.22	72.94	0.010	0.006

saving many computational efforts for MCM with $\sigma = 2$. One is the explicitness of each time step and the other is the unconditional stability. The explicitness of each time step allow MCM with $\sigma = 2$ involve no nonlinear iterations and the unconditional stability allow it select a time step without considering the upper stability limit.

Either the 5th or 6th column reveals that the ratio of the CPU time consumed by MCM with $\sigma = 2$ over that consumed by NEM or AAM is decreased with the increase of the total number of the degree of freedom. This implies that the computational efficiency of MCM with $\sigma = 2$ becomes more significant for a system with a large number of the degree of freedom when compared to NEM and AAM. Both the 5th and 6th columns show that the ratio of the CPU time might be as small as 1% or even smaller and thus the saving of computational efforts is very significant for MCM with $\sigma = 2$.

8. CONCLUSIONS

It has been shown that CEM has unconditional stability for a linear elastic system and any instantaneous stiffness softening system while for any instantaneous stiffness hardening system it can only have conditional stability. Thus, its applications to a general structural dynamic problem, where the total response is dominated by low frequency modes and the high frequency responses are of no interest, might be inconvenient or limited if an instantaneous stiffness hardening system is solved. In order to enhance the stability properties of CEM, the initial tangent stiffness is multiplied by an amplification factor and then used to determine the coefficients of the difference equation for displacement increment. As a result, MCM is obtained. In general, the numerical properties of MCM with $\sigma = 2$ inherit from CEM. The most important improvement is to extend stability range from $\delta_{i+1} \le 1$ for CEM to $\delta_{i+1} \le \sigma$ for MCM with a given value of σ. It is recommended that the choice of $\sigma = 2$ is appropriate for practical applications since it has an adequate unconditional stability range with an acceptable numerical accuracy. Thus, MCM with $\sigma = 2$ is best suited to solving a general structural dynamic problem since it is of no need to consider the stability problem in selecting an appropriate time step. This is because that it is very rare to experience an actual structural system, whose instantaneous degree of nonlinearity will be greater than 2. MCM with $\sigma = 2$ is also illustrated to be computationally efficient in the solution of a general structural dynamic problem. In fact, the CPU time consumed by MCM with $\sigma = 2$ might be less than 1% of those consumed by NEM and AAM.

ACKNOWLEDGEMENTS

The author is grateful to acknowledge that this study is financially supported by the National Science Council, Taiwan, R.O.C., under Grant No. NSC-99-2221-E-027-029.

REFERENCES

1. Newmark, N. M., "A Method of Computation for Structural Dynamics," *Journal of Engineering Mechanics Division*, ASCE, **85**, pp. 67–94 (1959).
2. Shing, P. B. and Mahin, S. A., "Elimination of Spurious Higher-Mode Response in Pseudo- Dynamic Tests," *Earthquake Engineering and Structural Dynamics*, **15**, pp. 425–445.
3. Chang, S. Y. "Improved Numerical Dissipation for Explicit Methods in Pseudodynamic Tests," *Earthquake Engineering and Structural Dynamics*, **26**, pp. 917–929 (1997).
4. Chang, S. Y., "The γ-Function Pseudodynamic Algorithm," *Journal of Earthquake Engineering*, **4**, pp. 303–320 (2000).
5. Houbolt, J. C., "A Recurrence Matrix Solution for the Dynamic Response of Elastic Aircraft," *Journal of the Aeronautical Sciences*, **17**, pp. 540–550 (1950).
6. Wilson, E. L., Farhoomand, I. and Bathe, K. J., "Nonlinear Dynamic Analysis of Complex Structures," *Earthquake Engineering and Structural Dynamics*, **1**, pp. 241–252 (1973).
7. Park, K. C., "An Improved Stiffly Stable Method for Direct Integration of Nonlinear Structural Dynamic Equations," *Journal of Applied Mechanics*, **42**, pp. 464–470 (1975).
8. Hilber, H. M., Hughes, T. J. R. and Taylor, R. L., "Improved Numerical Dissipation for Time Integration Algorithms in Structural Dynamics," *Earthquake Engineering and Structural Dynamics*, **5**, pp. 283–292 (1977).
9. Wood, W. L. Bossak, M. and Zienkiewicz, O. C., "An Alpha Modification of Newmark's Method," *International Journal for Numerical Methods in Engineering*, **15**, pp. 1562–1566 (1981).
10. Chung, J. and Hulbert, G. M., "A Time Integration Algorithm for Structural Dynamics with Improved Numerical Dissipation: The Generalized-α Method," *Journal of Applied Mechanics*, **60**, pp. 371–375 (1993).
11. Chang, S. Y., "A Series of Energy Conserving Algorithms for Structural Dynamics," *Journal of the Chinese Institute of Engineers*, **19**, pp. 219–230 (1996).
12. Chang, S. Y., "Improved Explicit Method for Structural Dynamics," *Journal of Engineering Mechanics*, ASCE, **133**, pp. 748–760 (2007).
13. Belytschko, T. and Hughes, T. J. R., *Computational*

https://doi.org/10.1017/jmech.2012.103 Published online by Cambridge University Press

Methods for Transient Analysis, Elsevier Science Publishers, B. V., North-Holland (1983).
14. Hughes, T. J. R., *The Finite Element Method*, Prentice-Hall, Inc., Englewood Cliffs, N. J., U.S.A. (1987).
15. Zienkiewicz, O. C., *The Finite Element Method*, McGraw-Hill Book Co (UK) Ltd. Third Edition (1977).
16. Goudreau, G. L. and Taylor, R. L., "Evaluation of Numerical Integration Methods in Elasto- Dynamics," *Computer Methods in Applied Mechanics and Engineering*, **2**, pp. 69–97 (1972).
17. Hilber, H. M. and Hughes, T. J. R., "Collocation, Dissipation, and 'Overshoot' for Time Integration Schemes in Structural Dynamics," *Earthquake Engineering and Structural Dynamics*, **6**, pp. 99–118 (1978).
18. Clough, R. W. and Penzien, J., *Dynamics of structures*, McGraw-Hill, Inc., International Editions (1993).
19. Bathe, K. J., "Finite Element Procedure in Engineering Analysis," *Prentice-Hall*, Inc., Englewood Cliffs, N.J., U.S.A. (1996).
20. Chang, S. Y., "Accuracy of Time History Analysis of Impulses," *Journal of Structural Engineering*, ASCE, **129**, pp. 357–372 (2003).
21. Chang, S. Y., "Accurate Representation of External Force in Time History Analysis," *Journal of Engineering Mechanics*, ASCE, **132**, pp. 34–45 (2006).
22. Chang, S. Y., Hsu, C. W. and Chen, T. W., "Comparison of Capability of Time Integration Methods in Capturing Dynamic Loading," *Earthquake Engineering and Engineering Vibration*, **9**, pp. 409–423 (2010).
23. Krieg, R. D., "Unconditional Stability in Numerical Time Integration Methods," *Journal of Applied Mechanics*, **40**, pp. 417–421 (1973).

(Manuscript received October 16, 2011,
accepted for publication February 7, 2012.)

https://doi.org/10.1017/jmech.2012.103 Published online by Cambridge University Press